A Novel SiNW/CMOS Hybrid Biosensor for High Sensitivity/Low Noise

Jieun Lee[1], Seonwook Hwang[1], Bongsik Choi[1], Jung Han Lee[2], Dong-Il Moon[3], Myeong-Lok Seol[3], Chang-Hoon Kim[3], In-Young Chung[4], Byung-Gook Park[2], Yang-Kyu Choi[3], Dong Myong Kim[1], Dae Hwan Kim[1], and Sung-Jin Choi[1*]

[1]EE, Kookmin University, Korea, [2]EECS, Seoul National University, Korea,
[3]EE, KAIST, Korea, [4]ECE, Kwangwoon University, Korea,
Email: [*]sjchoiee@kookmin.ac.kr, Phone: +82-2-910-5543, Fax: +82-2-910-4449

Abstracts

A novel silicon nanowire (SiNW)/CMOS hybrid biosensor was produced for the first time. The hybrid biosensor features a complementary SiNW block and CMOS logic inverter readout circuitry. The proposed hybrid biosensor shows remarkably sensitive output voltage (Δ1.2 V/Δ0.4 pH and Δ1.2 V/Δ200 fM DNA) without noise or fluctuations.

1. Introduction

Silicon nanowires (SiNWs) show outstanding potential in biosensor applications due to their high sensitivity, real-time label-free detection capabilities and low cost [1]. Several types of SiNW biosensors have been proposed to improve sensor performance [2-3]. However, the actual performance of readout circuitry has not been effectively improved (Fig. 1). Moreover, noise or fluctuations may be amplified in these structures (Fig. 1). Thus, the implementation of highly sensitive SiNW biosensor circuitry and the elimination of noise are significant challenges. In the present work, we propose a novel top-down SiNW/CMOS hybrid biosensor circuitry with two functional stages (Fig. 2). The 1st stage consists of a series-connected complementary (n-/p-type) SiNW block, which senses the target biomolecules and amplifies the bio-signal, yielding high sensitivity. The 2nd stage is composed of a CMOS circuit block, which further amplifies the bio-signal and eliminates noise without sacrificing sensitivity.

2. Experimental

The proposed SiNW/CMOS hybrid biosensor was fabricated on a 6” silicon-on-insulator (SOI) wafer using conventional CMOS technology. The SiNWs and CMOS active regions were formed on the top silicon layer using an electron-beam (e-beam) mix-and-match process combined with conventional photolithography. The fabrication process is illustrated in Fig. 3. The monolithic integration of the SiNWs and CMOS circuit was successfully achieved, as shown in Fig. 4. Cross-sectional transmission electron microscopy images of the SiNW channel and the experimental setup are displayed in Fig. 5. The sensing responses of the SiNW/CMOS hybrid biosensor circuitry were characterized for solutions with different pHs and DNA hybridizations using a semiconductor parameter analyzer (4156C, Agilent) at room temperature. Over 99% of the integrated SiNWs were successfully built within the design specifications shown in Fig. 6.

3. Results and Discussion

3.1 pH response of SiNW FETs

Fig. 7 shows the measured transfer characteristics of n- and p-type SiNW FETs for five different pH values. As shown in Fig. 8, the threshold voltage (V_{TN} /V_{TP} for n-/p-types) shift with respect to the change in pH was less than 59.6 mV at room temperature, which is in accordance with the well-known Nernst limit [4].

3.2 Signal amplification

Fig. 9 shows the voltage transfer curves (VTC) of the proposed SiNW/CMOS hybrid biosensor for different pH levels. The logic threshold voltage (V_{LT}) shifted in the positive direction as the pH increased. The SiNW surface became negatively charged due to an increase in the pH; as a result, a positive shift in V_{TN} was observed for the n-type SiNW FET, and a negative shift in V_{TP} occurred for the p-type SiNW FET, which shifted V_{LT}. Therefore, our proposed biosensor can be operated at different pH levels. The measured V_{LT} shift was 53.5 mV/pH, which is similar to the Nernst limit, as shown in Fig. 9. As a new sensing metric, the output voltage shift per pH change in the 1st stage ($\Delta V_{OUT1}/\Delta pH$) can be amplified as high as the voltage gain (A_{V1}) by the complementary SiNW block, compared to $\Delta V_{LT}/\Delta pH$ (i.e., the Nernst limit) (Fig. 10). Moreover, the final output voltage shift in the 2nd stage ($\Delta V_{OUT2}/\Delta pH$) can be further amplified by multiplexing A_{V1} and A_{V2} (voltage gain in CMOS circuit). The transient output voltage (V_{OUT2} versus time) due to different pH levels demonstrates that pH changes result in a clear and amplified binary signal, i.e., Δ1.2 V(V_{DD2})/ΔpH, as shown in Fig. 11. Three different types of sensing readout circuitry for the detection of pH levels are compared in Fig. 12. The sensitivity of the output voltage in the proposed SiNW/CMOS hybrid biosensor was approximately 4 times greater than that of single SiNW circuitry (Fig. 12). Therefore, we expect that highly sensitive output voltage signals due to minor changes in the pH (Δ0.1 pH) can also be achieved in our structure, as simulated in Fig. 13. The experimental results verified that the proposed biosensor outperforms conventional biosensors (Fig. 14). A small change in pH can be successfully detected with high sensitivity (Δ1.2 V/Δ0.4 pH), which indicates that the high sensitivity of the biosensor circuitry to pH changes can be translated to enhanced sensitivity in other biomolecule detections.

3.3 Noise reduction

Due to its hybrid structure, we can also reject noise and voltage fluctuations from the electrolyte bulk and the electrolyte oxide interface. Fig. 15(a) shows the basic principles of noise cancellation in the SiNW/CMOS hybrid biosensor. Because the 2nd stage CMOS circuit was located next to the 1st stage of the biosensor, noise can be rejected due to the inherent characteristics of the inverter chain. The experimental and TCAD simulation results confirmed that noisy bio-signals were clearly eliminated in the proposed biosensor, as shown in Figs. 15 (b) and (c). Therefore, the proposed biosensor can produce highly sensitive bio-signals without noise or fluctuations.

3.4 DNA detection

To detect DNA using the proposed structure, the electrostatic immobilization method was adopted to functionalize the SiNW surface (Fig. 16) [5]. Complementary target DNA hybridization induces a noticeable positive V_{LT} shift due to the negative charge of DNA sequences, whereas the non-complementary target DNA induces only a negligible V_{LT} shift (Fig. 17 and 18). Furthermore, the 1 pg/ml (= 200 fM) complementary target DNA noticeably changes the 2nd stage output voltage (ΔV_{OUT2} ~ 1.2 V) due to bio-signal amplification and noise rejection in our biosensor, as shown in Fig. 19. Therefore, the proposed biosensor presents extremely high sensitivity for label-free DNA detection.

3.5 Operating region for improved sensor performance

We evaluated the performance of the proposed biosensor circuitry by changing the operating regions of n- and p-type SiNW FETs in the 1st stage using a Monte Carlo SPICE simulation, including subthreshold, saturation, and linear regions. As shown in Fig. 20, because the current sensitivity of the single SiNW was maximized in the subthreshold region, the voltage gain was maximized when the SiNW/CMOS hybrid biosensor was operated in the subthreshold region (Fig. 21). In addition, we simulated the variation of the voltage gain using the undesired threshold voltage shift due to process uncertainties at each operating region and confirmed that variations in sensitivity can also be reduced in the subthreshold region. Therefore, the total sensitivity is enhanced and process variation is reduced by optimizing the operating region.

4. Conclusion

We presented a novel SiNW/CMOS hybrid biosensor and showed that monolithic co-integration with SiNWs and CMOS readout circuit was feasible. The proposed biosensor showed excellent sensor performance and can reduce noise/fluctuations without impairing performance. In addition, we confirmed that the sensitivity and process variability can be maximized and minimized, respectively, by adjusting the operating region of the biosensor. Therefore, our designed hybrid sensor is an ideal candidate for autonomous sensor applications.

Acknowledgments

This work was supported by the National Research Foundation of Korea (NRF) grant, which is funded by the Korea government (Grant No. 2009-0080344, No. 2010-0027649, and No. 2013R1A2A2A05005472), BK21+, and the Center for Integrated Smart Sensors, which is funded by the Ministry of Science, ICT & Future Planning through the Global Frontier Project (CISS-2012M3A6A6054187).

References

[1] E. Stern, James F. Klemic, David A. Routenberg, Pauline N. Wyrembak, Daniel B. Turner-Evans, Andrew D. Hamilton, David A. LaVan, Tarek M. Fahmy, and Mark A. Reed, "Label-free immunodetection with CMOS -compatible semiconducting nanowires," *Nature*, vol. 445, no.1, pp. 519-522, Feb. 2007.

[2] O. Knopfmacher, A. Tarasov, Wangyang Fu, M. Wipf, B. Niesen, M. Calame, and C. schönenberger, "Nernst Limit in Dual-Gated Si-Nanowire FET Sensors," *Nano Lett*., vol. 10, no. 6, pp. 2268-2274, May 2010.

[3] R. A. Chapman, Richard A. Chapman, Poornika G. Fernandes, Oliver Seitz, Harvey J. Stiegler, Huang-Chun Wen, Yves J. Chabal, and Eric M. Vogel, "Comparison of Methods to Bias Fully Depleted SOI-Based MOSFET Nanoribbon pH Sensors," *IEEE Trans. on Electron Devices*, vol. 58, no. 6, pp. 1752-1760, June 2011.

[4] L. Bousse, Nico F. De Rooij, and P. Bergveld, "Operation of chemically sensitive field-effect sensors as a function of the insulator-electrolyte interface," *IEEE Trans. on Electron Devices*, vol. 30, no. 10, pp. 1263-1270, 1983.

[5] J.-H Ahn, J.-Y. Kim, C. Jung, D.-I. Moon, S.-J. Choi. C.-H. Kim, K.-B. Lee, H. G. Park, and Y.-G. Choi, "CMOS -based biosensors with an independent double-gate FinFET," *IEDM 2011*, p 36.2.1-36.2.4, Dec. 2011.

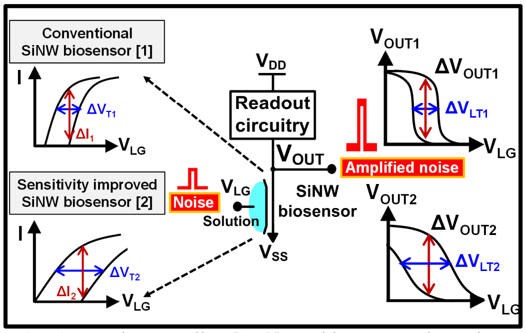

Fig. 1: Previous studies [1, 2] on biosensors showed an increase in the V_T shift, but the current sensitivity did not change ($\Delta V_{T1} < \Delta V_{T2}$, $\Delta I_1 = \Delta I_2$ [3]). Accordingly, the output voltage sensing margin in the actual readout circuitry did not improve ($\Delta V_{OUT1} = \Delta V_{OUT2}$). Moreover, noise or fluctuations could be amplified.

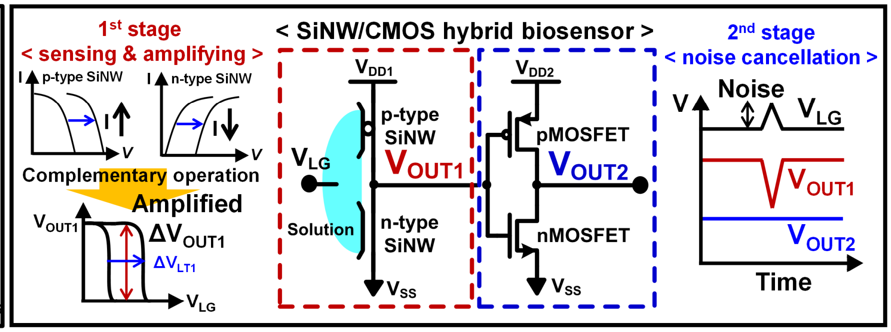

Fig. 2: The proposed SiNW/CMOS hybrid biosensor for signal amplification and noise cancellation. (1st stage) ΔV_{OUT1} is amplified by the series-connected complementary SiNW block. (2nd stage) The CMOS circuit further amplifies the bio-signal and eliminates noise without reducing the sensitivity.

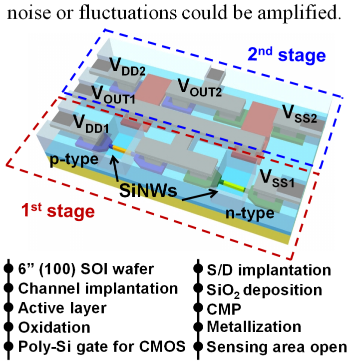

Fig. 3: Process flow of the SiNW/CMOS hybrid biosensor on a SOI wafer.

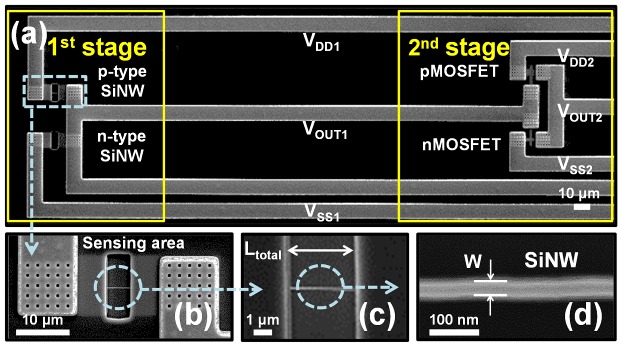

Fig. 4: Scanning electron microscopy images of (a) the SiNW/CMOS hybrid biosensor. (b) A SiNW biosensor in the 1st stage. (c) Magnified view (L_{total} = 4 μm). (d) SiNW channel region.

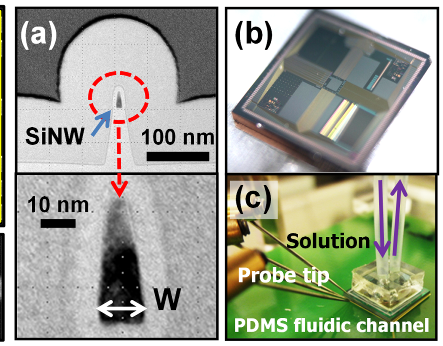

Fig. 5: (a) Transmission electron microscope images of the SiNW. (b) Photo of the fabricated chip and (c) the experimental set-up.

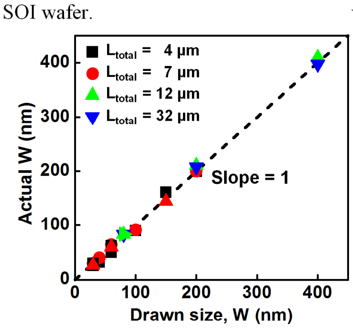

Fig. 6: SiNW W versus the actual SiNW W of fabricated SiNWs on a SOI wafer. The actual SiNW W was extracted from the SEM images.

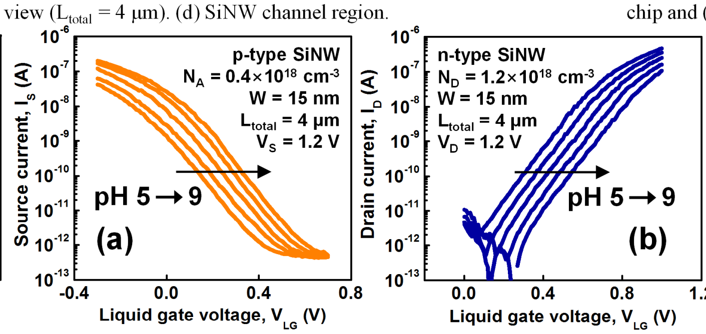

Fig. 7: Transfer characteristics of (a) p-type and (b) n-type SiNW FETs for different pH levels (0.1 M potassium phosphate buffer, pH 5 - 9). An Ag/AgCl reference electrode was employed as the liquid gate voltage (V_{LG}) electrode. As the pH changed, a clear threshold voltage shift and current modulation was observed for both n- and p-type FETs.

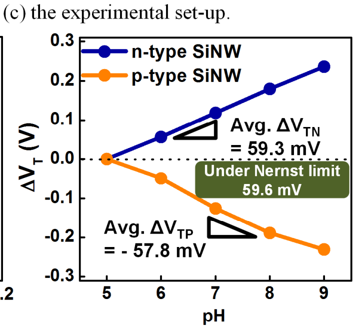

Fig. 8: Threshold voltage shift (ΔV_T) with respect to pH changes for both n- and p-type SiNW FETs. The average ΔV_T per pH remained below the Nernst limit (59.6 mV/pH @ T = 300 K).

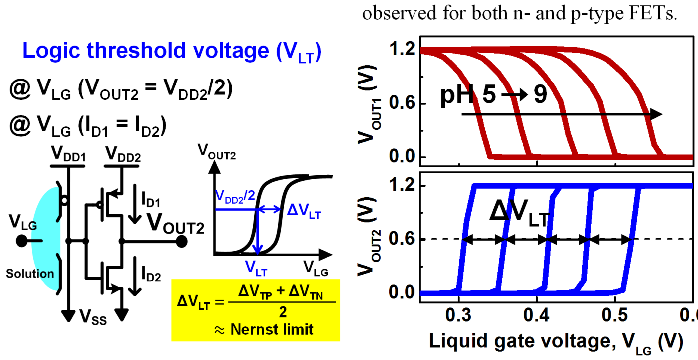

Fig. 9: (Left) Definition of the logic threshold voltage (V_{LT}) and its influence on the threshold voltage shift due to pH changes. (Right) Measured voltage transfer curves of the SiNW/CMOS hybrid biosensor for different pH levels (W = 15 nm, L_{total} = 4 μm, $V_{DD1} = V_{DD2}$ = 1.2 V). The average ΔV_{LT} was 53.5 mV.

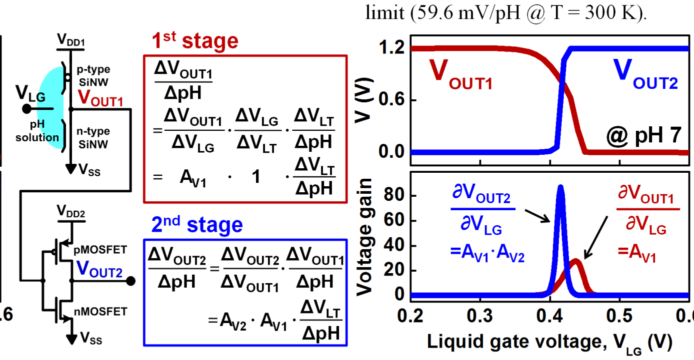

Fig. 10: (Left) Output voltage sensitivity of the 1st and 2nd stages of the SiNW/CMOS hybrid biosensor. (Right) Measured voltage transfer curves and extracted voltage gains of the SiNW/CMOS hybrid biosensor.

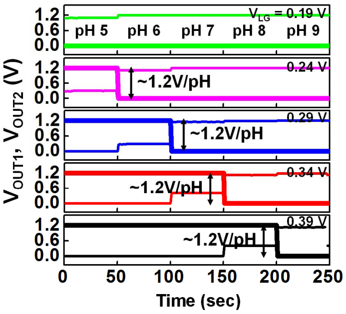

Fig. 11: Transient responses of the output voltages due to changes in the pH level in the SiNW/CMOS hybrid biosensor (thick line: V_{OUT2}, thin line: V_{OUT1}).

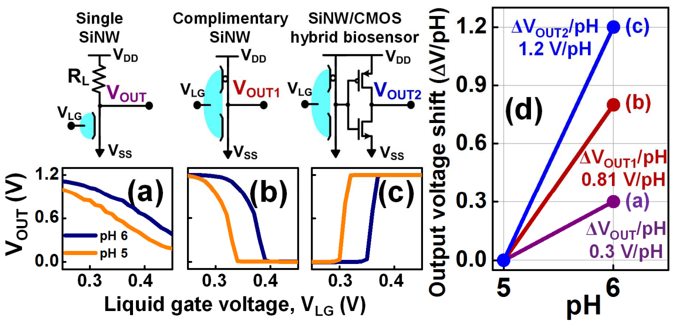

Fig. 12: Voltage transfer curves of (a) the resistive load type (single SiNW), (b) complementary SiNW block (1st stage), and (c) SiNW/CMOS hybrid biosensor (1st and 2nd stages). (d) A comparison of output voltage sensitivities in three types of biosensors (V_{DD} = 1.2 V).

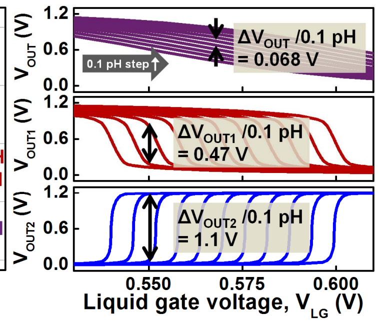

Fig. 13: Simulated results of the voltage transfer curves of three types of biosensors (Fig. 12) due to pH changes in increments of 0.1 units.

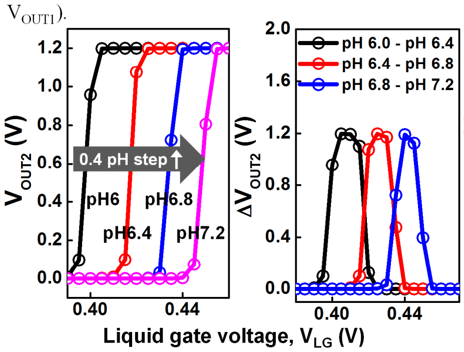

Fig. 14: Measured voltage transfer curves of the SiNW/CMOS hybrid biosensor for different pH values in increments of 0.4 units. The averaged ΔV_{OUT2}/0.4 pH was approximately 1.2 V.

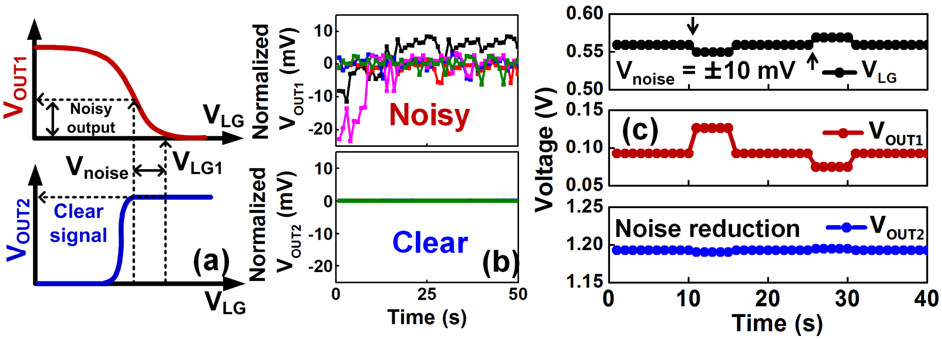

Fig. 15: (a) Schematic depiction of noise cancellation in the SiNW/CMOS hybrid biosensor. (b) The experimental results showed that the noisy V_{OUT1} was clearly transformed into the noiseless signal in V_{OUT2}. (c) The simulated transient output voltage response of the SiNW/CMOS hybrid biosensors. Noise voltage (V_{noise}) was added to V_{LG} for 5 sec. The black arrows represent the time at which noise was inserted.

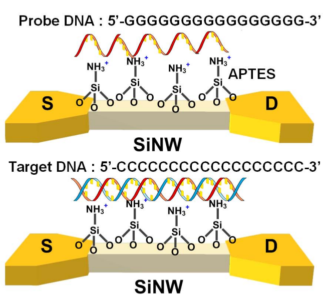

Fig. 16: Experimental procedures for DNA detection using the electrostatic immobilization method.

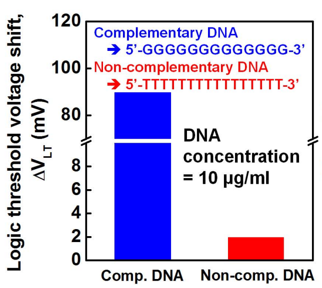

Fig. 17: Logic threshold voltage shift of the complementary/non-complementary DNA-hybridized SiNW/CMOS hybrid biosensor.

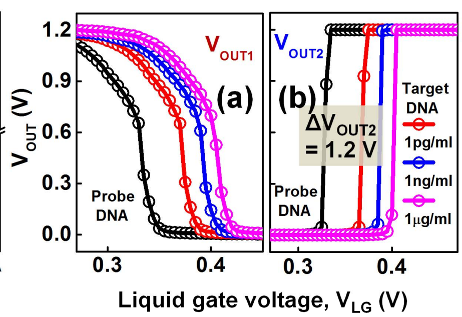

Fig. 18: Voltage transfer curves of (a) the 1st stage and (b) 2nd stage of the DNA-hybridized SiNW/CMOS hybrid biosensor (1 pg/ml = 200 fM). The target DNA sequence induced a positive V_{LT} shift.

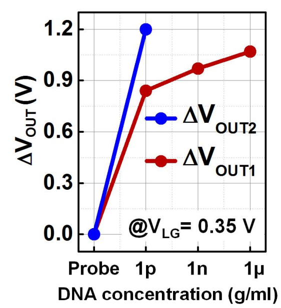

Fig. 19: Output voltage shift of the target DNA-hybridized SiNW/CMOS hybrid biosensor.

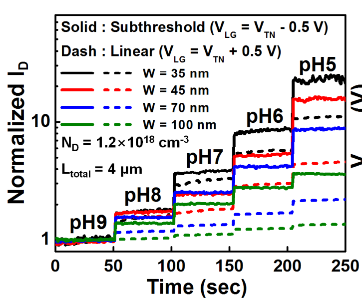

Fig. 20: Transient response of the drain current (I_D) in n-type SiNW FETs with various widths for different operating regions (pH: 5-9).

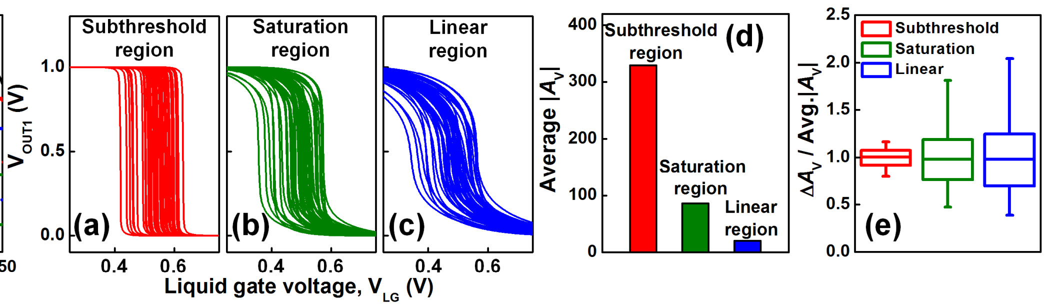

Fig. 21: Simulated voltage gain of the 1st stage of the SiNW/CMOS hybrid biosensor (SPICE Monte Carlo simulation). The maximum allowed mismatch value for ΔV_{TN} and ΔV_{TP} was 200 mV, and the number of events was set to 100. The operating region in: (a) the subthreshold region ($V_{TN} > V_{DD}/2$, $-V_{TP} > V_{DD}/2$) (b) the saturation region ($0 < V_{TN} < V_{DD}/2$, $0 < |V_{TP}| < V_{DD}/2$, and $V_{TP} < 0$), and (c) under linear conditions ($V_{TN} < 0$, $0 < V_{TP}$). (d) The average voltage gain for each region. Operation in the subthreshold region led to the maximum average voltage gain. (e) ΔA_V/Avg.$|A_V|$ indicated that operation in the subthreshold region was the most robust with respect to process variability.